ISSN 0915-633X

NATIONAL INSTITUTE FOR FUSION SCIENCE

Innovative Direct Energy Conversion Systems from Fusion Output Thermal Power to the Electrical One with the Use of Electronic Adiabatic Processes of Electron Fluid in Solid Conductors.

Y. Kondoh, M. Kondo, K. Shimoda, T. Takahashi and K. Osuga

(Received - June 12, 2003)

NIFS-776 July 2003

TOKI, JAPAN

Innovative Direct Energy Conversion Systems from Fusion Output Thermal Power to the Electrical One with the Use of Electronic Adiabatic Processes of Electron Fluid in Solid Conductors

Y. Kondoh, M. Kondo, K. Shimoda, T. Takahashi, and K. Osuga
Dept. of Electronic Engineering, Gunma University,
Kiryu, Gunma 376-8515, Japan
kondohy@el.gunma-u.ac.jp, http://www.el.gunma-u.ac.jp/~t-tak/index.html
†Patent application number, Patent Agency of Japan:2001-172963,
2002-167059, PCT/JP/05679

Abstract

. It is shown that with the use of the fusion output and/or environmental thermal energy, innovative open systems for permanent auto-working (PA) direct energy converting (DEC) from the thermal to the electrical (TE) and further to the chemical potential (TEC) energies, abbreviated as PA-TEC-DEC systems, can be used for new auto-working electrical power plants and the plants of the compressible and conveyable hydrogen gas resources at various regions in the whole world. It is analytically shown that the same physical mechanism by free electrons and electrical potential determined by temperature in conductors, which include semiconductors, leads to the Peltier effect and the Seebeck one. It is analytically proved that the energy conservation law is exactly satisfied in a simple form where the net absorbed thermal power is directly transferred to the electrical power and to the chemical power in the PA-TEC-DEC systems. It is analytically and experimentally clarified that the long distance separation between two π type elements of the heat absorption side and the production one of the Peltier effect circuit system or between the higher temperature side and the lower one of the Seebeck effect circuit one does not change mechanisms of the heat pumping by the Peltier effect and of the TE-DEC by the Seebeck effect. The proposed systems gives us freedom of no using the fossil fuel, such as coals, oils, and natural gases that yield serious greenhouse effect all over the earth, and the plant of nuclear fissions that left radiating wastes, i.e., no more environmental pollutions. The PA-TEC-DEC systems can be applicable for several km scale systems to the micro ones, such as the plants of the electrical power and the hydrogen gas resources, compact transportable hydrogen gas producers, the refrigerators, the air conditioners, home electrical apparatuses, and further the computer elements.

Keywords: electronic adiabatic process, electronic heat pumping, free electron fluids in conductors, direct energy conversion system from fusion thermal output, direct thermal-chemical potential energy conversion system, permanent auto-working (PA) electrical power plant, PA plants of hydrogen gas resources, open systems

PACS numbers: 84.60.Rb, 84.90.+a, 89.30.+g, 89.90.+n

I. INTRODUCTION

It has been attracted the scientific research that the fossil fuel, such as the oil and the natural gas, would be consumed out within several tens years from the earth for these several years. The electric power plants using the nuclear fission have inevitable feature of radioactive dust and dangerous running without control by careless accidents. On the other hand, the power plants using the nuclear fusion have many advantages compared with the fission plant, such as the low neutron yields to suppress the radioactive dust and naturally shutdown because of cooling of confined plasmas. Various types of confinement system for the fusion plants have been proposed hitherto, such as the Tokamak, Stellarator, Tandem Mirror, Reversed Field Pinches (RFP), Field Reversed Configurations (FRC), Compact Torus (CT), Spherical Tokamak (ST), and so on. In the case of the RFP, the self-organization process has been known to lead to the stable state of the confined plasma. Many theories to interpret the self-organization phenomena in plasmas have been proposed, and one of the authors have been contributed for the

development of this research area [1-9]. The present authors have also reported systems of direct energy converter from thermal to electrical and further to chemical potential energies [10]. The fusion output power is usually converted to the thermal power at the blanket, and the water is a candidate to absorb the thermal power for establishment of the usual electrical power plant. In order to reduce radioactive dust produced at the blanket, we have to develop some other systems of direct energy converter from thermal to electrical and further to chemical potential energies. On the other hand, research works on the scientific analysis, the application, the industrialization concerning to the Peltier effect and Seebeck one have been published a lot in various journals [11-16].

In this paper, we present innovative open systems of direct energy conversion using electronic adiabatic processes of electron fluid in solid conductors, i.e., new plants of electrical power and hydrogen gas resources from the output of fusion energy. In Section II, we present the theoretical background and some data by demonstrative experiments for the innovative direct energy conversion systems. Sections II-1 and II-2 are for the Peltier effect and the Seebeck one, with circuit equations and demonstrative experimental data. Section II-3 is for the electronic heat pumping (EHP) with circuit equations and demonstrative experimental data, and some proposal of a auto-working EHP system, new plants of electrical power and the conveyable hydrogen gas resources, without environmental pollutions. We have obtained some experimental evidence such as the conveyable hydrogen gas by a preliminary experiment on the resolving water system. Concluding remarks are in Section IV.

II. THEORETICAL BACKGROUND AND EXPERIMENTS WITH DISCUSSION

We present here a theoretical background for electronic adiabatic processes of free electron fluids in solid conductors, which include semiconductors, and demonstrative experiments with discussion.

II-1. Energy transfers between thermal energies and electrical potential ones of free electrons by electronic adiabatic process

At first, we consider an energy band diagram around contact surfaces among three conductors A, a metal M, and B with external electric field from B side to A one, as schematically shown in Fig. 1. Here, A and B are conductors with large absolute thermoelectric power, called the (absolute) Seebeck coefficient written as $\alpha_A(T_1)$ and $\alpha_B(T_1)$, respectively. The value of the Seebeck coefficient of the metal M such as the copper Cu is usually very small compared with A and B. The Seebeck coefficient depends on the temperature T_1 around contact surfaces. The Fermi energy level is denoted by E_F, the lowest level of the conduction band by E_C, the highest level of the valence band by E_V, and the vacuum level by E_{VAC}. Since the heat conduction is high enough around the two contact surfaces in Fig. 1, the temperature of A, M, and B become respectively the same temperature T_1 as a result. Since the external electric field is applied from B to A, the Fermi level E_F is the highest in A, the middle in M, and the lowest in B. The free electron distributions in semiconductors and metals can be usually expressed respectively by the Boltzmann distribution and the Fermi-Dirac one. The electrical potential $\phi_A(T_1)$ and $\phi_B(T_1)$ are measured from the vacuum level E_{VAC} to the E_F level, and the threshold energy for electrons to go out from conductors is given by E_{VAC} - E_F. The potential difference $V_{BA}(T_1)$ between B side and A one is given by

$$V_{BA}(T_1) = \phi_B(T_1) - \phi_A(T_1). \qquad (1)$$

We use the two conductors of A and B in which electrical potentials have the features of $\phi_B(T_1) > \phi_A(T_1)$. On the other hand, $V_{BA}(T_1)$ has the following experimental relation with the use of the relative thermoelectric power (i.e., relative Seebeck coefficient) $\alpha_{BA}(T_1)$, as follows

$$V_{BA}(T_1) = \alpha_{BA}(T_1)T_1 \equiv \alpha_{BAT1}T_1 > 0, \qquad (2)$$

where $\alpha_{BA}(T_1)$ is hereafter abbreviated as α_{BAT1}, and is written by the Seebeck coefficient $\alpha_A(T_1)$ and $\alpha_B(T_1)$ as

$$\alpha_{BAT1} = \alpha_B(T_1) - \alpha_A(T_1), \qquad (3)$$

From Eqs.(1) and (2), we obtain

$$\alpha_{BAT1} = [\phi_B(T_1) - \phi_A(T_1)]/T_1. \quad (4)$$

From Eq. (4), we see the relation of $\alpha_{BAT1} = -\alpha_{ABT1}$. Electrons in the conduction band and the valence one, where in the latter band electrons move reversely against the holes of positive carrier, have their own total energy H written by

$$H = e\phi(T_1) + \frac{m_e}{2} v_{fi}^2, \quad (5)$$

where $(m_e/2)\, v_{fi}^2$ denotes the kinetic thermal energy of the every free electrons.

We now consider the electronic adiabatic process of the free electrons in the conduction band and electrons in the valence band around the contact surfaces between A and M, and between M and B, shown in Fig. 1. At first, we pay our attention to all electrons in the conduction band and the valence one. When every free electrons are driven from A to B (the direction of current is inversely from B to A) by external electric fields, they move adiabatic from A to M and M to B through the two contact surfaces, keeping their total energy H, as follows

$$\begin{aligned} H &= e\phi_A(T_1) + \frac{m_e}{2} v_{fiA}^2 \\ &= e\phi_M(T_1) + \frac{m_e}{2} v_{fiM}^2 \\ &= e\phi_B(T_1) + \frac{m_e}{2} v_{fiB}^2 \end{aligned} \quad (6)$$

where v_{fiA} denotes the kinetic velocity of every free electrons of interest, which were in A, and v_{fiB} is that of the same free electrons which have moved into B. Here, the drift velocity of free electrons by the external electric field can usually be negligible compared with the thermal velocity in the conductors, and therefore the kinetic energy of the free electron by the drift velocity accompanied by external electric fields is neglected in Eq.(6). From the electronic adiabatic equation (6), we obtain the followings:

$$\frac{m_e}{2} v_{fiA}^2 - \frac{m_e}{2} v_{fiM}^2 = e[\phi_M(T_1) - \phi_A(T_1)], \quad \frac{m_e}{2} v_{fiM}^2 - \frac{m_e}{2} v_{fiB}^2 = e[\phi_B(T_1) - \phi_M(T_1)], \quad (7)$$

$$\because \quad \frac{m_e}{2} v_{fiM}^2 = \frac{m_e}{2} v_{fiA}^2 - e[\phi_M(T_1) - \phi_A(T_1)], \quad \frac{m_e}{2} v_{fiB}^2 = \frac{m_e}{2} v_{fiM}^2 - e[\phi_B(T_1) - \phi_M(T_1)]$$

$$\therefore \quad \frac{m_e}{2} v_{fiB}^2 < \frac{m_e}{2} v_{fiM}^2 < \frac{m_e}{2} v_{fiA}^2, \quad (8)$$

where $\phi_B(T_1) > \phi_M(T_1) > \phi_A(T_1)$. From Eq. (7), we can find a physical fact that through the electronic adiabatic process (EAP) of the free electrons from A to M and from M to B, the kinetic thermal energy of the free electrons of interest have been converted to the electrical potential energy by passing through the two contact surfaces with M. In this way, the direct energy converting (DEC) from the thermal to the electrical energies (TE) is realized through the electronic adiabatic process (EAP) of free electrons, abbreviated as the TE-DEC by the EAP. We can see from Eq.(8) that the kinetic thermal energy of the free electrons of interest has become lower by passing through the contact surfaces. Therefore, the heat absorption takes place in the M side neighbor of the contact surface with A and also in the B side one with M due to the long range Coulomb force interaction among the free electrons, which have flowed in, and those that have existed in M and B before hand by quite short equi-partition time of kinetic energies. When a long cable conductor is attached to the B side, the Coulomb interaction travels along the cable conductor with the speed of electromagnetic waves (EMW). The traveling time of the EMW is greatly shorter due to the light velocity and this time is quite smaller than the equi-partition one due to a lot of interactions among electrons.

Equi-partiton time between the injected free electrons and positive atoms is the largest one in the M and B sides. If the external electric field to drive free electrons is reversed, the level of E_F in the side of A, M, and B becomes highest in B, middle in M, and lowest in A. Since the threshold energy $E_{VAC} - E_F$ does not change by the reversal of the external electric field, the electrical potential remains as $\phi_A(T_1) < \phi_M(T_1) < \phi_B(T_1)$ in Eq. (7). In this case of reversed external electric field, the heat production takes place in the M side neighbor of the contact surface with B and also in the A side one with M, consequently. This TE-DEC by the EAP in conductors is the fundamental physical mechanism of the well-known Peltier effect elements having the structure of [A(T_1), M, B(T_1)] or simply [A(T_1), B(T_1)].

Following experimental fact must be emphasized here for the Peltier circuit with a pair of heat absorption and production sides, using two π type Peltier elements: If the heat sink material attached to the heat production side A(p), which means a p type semiconductor, is not enough to take out the produced thermal energy, then all parts of A(p), M, and B(n) in Fig. 1 become to have equal and very high temperature T_1 due to their high heat conduction. Because of the very high temperature, lots of electrons in the valence band are exited to the conduction band to make the E_F level quite high so that all electrical potentials become equal as $\phi_A(T_1) = \phi_M(T_1) = \phi_B(T_1)$. Consequently, the Peltier effect does not work any more in this situation, and the external electrical power is used only for Ohmic heating of the electrical resistance of Peltier effect elements. In other words, disappearance of the Peltier effect takes place in the experimental system. Because of this fact, all commercial products using the Peltier effect elements have large heat sink or heat radiation parts and/or electrical fans, at present. In order to avoid this problem mentions above, we proposed a novel and simple method by separating the two π type Peltier elements, one of which is the heat production side and the other is the absorption one, with the use of highly electrical conductive long wires in the open systems as shown in Fig. 2(a). Here, the two π type Peltier elements in Fig.2(a) have the pair of the endothermal side and the exothermal one as is shown in the figure. One of the important innovative facts included in this method is that the endothermal energy and the exothermal one are not canceled out within one set of π type Peltier elements, but they are canceled out between the exothermal side and the endothermal one, which are connected by highly electrical conductive long wires, as will be shown later by demonstrative experimental data.

On the other hand, the Seebeck effect elements have the same structure of [A(T_1), M, B(T_1)] or simply [A(T_1), B(T_1)]. If the temperature of conductors becomes higher, then the bounded electrons are released more to the free electrons to raise the level of E_F. Therefore, the electrical potential $\phi_A(T_1)$ becomes lower when T_1 is higher.. If we keep two temperatures of T_1 and T_2 as $T_1 > T_2$ like as shown in Fig. 2(a) for two mutually connected π type Peltier effect elements of [A(T_1), M, B(T_1)] and [A(T_2), M, B(T_2)], then we obtain the serial electrical potential difference $Vcn(T_1,T_2) = \{ [\phi_B(T_1) - \phi_M(T_1)] + [\phi_M(T_1) - \phi_A(T_1)] \} + \{ [\phi_A(T_2) - \phi_M(T_2)] + [\phi_M(T_2) - \phi_B(T_2)] \} = Vcn(T_1) + Vcn(T_2)$, which is known as induced voltage by the Seebeck effect. We may find from these facts that the Peltier effect and the Seebeck one come from the same physical mechanism embedded in conductors.

We have done demonstrative experiments using two set of three or five π type Peltier elements with two separations of about 1 cm and 225 cm, as shown in Fig.2 (b), where .the left and the right side sets of π type Peltier elements are connected as n-type to n-type and p-type to p-type in series. It is noted here that we use the cables connecting the both sides of the two Peltier effect circuit systems, which are made by conductors with quite high electrical conductivity. Figure 2 (c) shows experimental data for the case of about 1 cm separation between the two set of three π Peltier elements in Fig. 2 (b). The room temperature is kept to be around 24.0 ℃ for the experiment of Fig. 2 (c) and around 26.5 ℃ for the experiment of Fig. 2 (d). It is seen from Fig. 2 (c) that from the beginning to around 0.5 min, the temperature T_4 at the HAS goes down, but after the cooling down the value of T_4 goes up just like the curve of T_1 at the HPS. This experimental result indicates that the thermal conduction from the HPS to the HAS heats up the HAS to increase T_4 almost proportional to T_1 . Figure 2 (d) shows experimental data for the case of about 225 cm separation between the two set of five π Peltier elements in Fig. 2 (b), where error bars are shown on the data curves. It is seen from Fig. 2(d) that after the time of around 10.0 min, the value of T_4 at the HAS becomes to be steadily constant lower than the room temperature because of the thermal balance between the cooling Peltier effect and the warming by the surrounding air. The value of T_1 at the HPS is seen to gradually increases up to about 62.5 ℃ and the difference between T_1 and T_4 becomes about 40.0 ℃. The time evolution of T_1 and T_4 in Fig. 2(d) is seen to

be quite different from that in Fig. 2(c). Other interesting fact of the data in Fig. 2(d) is that the temperature T_2 at the endothermal side goes down until around 1.0 min and then gradually goes up to become close to the temperature T_3 at the exothermal side with difference of temperature around 4.5 ℃. Both values of T_2 and T_3 are higher than the room temperature of about 26.5 ℃ by around 10.0 ℃. The Joule heating by fairly high DC current of 5.0 A is considered to affect the temperatures of T_2 and T_3 to become higher than the room temperature. The most important point is that T_2 at the endothermal side and T_3 at the exothermal one become close to each other within a rather short time of around 15.0 min. In other words, the initial decreased kinetic energy of electrons that determines the value of T_2 and the increased one that determines the value of T_3 have almost cancelled out with each other within the time of about 15.0 min along the cupper wire cable length of about 225 cm, i.e., the approximate cancellation time t_{can} = 15.0 min. In order to check the possibility of cancellation due to the thermal diffusion and the electron drift velocity along the cable, we have measured the Ohm's drop along the 225 cm cable and have calculated the drift velocity of electrons. At first, we have measured whether the thermal diffusion along 225 cm cable reaches the other end during t_{can} = 15.0 min, and have found that the thermal diffusion time is much longer than 15.0 min. Second, using the mobility $\mu = 30$ [cm^2/V_0 (t·s)] of the cupper around room temperature and the electric field $E = 0.78 \times 10^{-3}$ (V/cm) obtained from dividing the Ohmic drop by 225 cm, we obtain the drift velocity $v_d = 0.23 \times 10^{-1}$ (cm/s). The transferred distance L_{tr} of thermal energy carried by drifting electrons during t_{can} = 15.0 min can be estimated as $L_{tr} = v_d \times 900$ s= 11.0 cm. We then find the fact that the distance L_{tr} =11.0 cm is much less than 225 cm of the cable, and therefore the drift velocity of electrons cannot be the physical candidate for the experimental cancellation time of t_{can} = 15.0. min. One of qualitative explanation is as follows: A huge amount of electrons that had flowed in the cupper cable from the semiconductor would induce electrical potential fluctuations in the cable, and the fluctuating potential would propagate along the cupper cable to the other end with the speed of electromagnetic wave in the cable. The propagating potential fluctuations, however, would reflect at the end and propagate back to the other direction, and the propagating potential fluctuations would repeat go and back along the cable until the fluctuating potential energies would have absorbed into the thermal energies of electrons, whose thermal energies would finally go into the thermal energies of cupper atoms to balance thermal energies between electrons and atoms. The physical mechanism to explain quantitvatively the short cancellation time t_{can} = 15.0 min, however, is still left behind for further theoretical and experimental investigations.

II-2. Applications of energy transfers between thermal energies and electrical potential ones by the electronic adiabatic process

Using the TE-DEC by the EAP, i.e., the Peltier effect, there have been developed the so-called heat pumping modules, which follow the usual gaseous heat pumping with the use of the adiabatic-compression and expansion of circulating gases, are commonly used in various devices such as computers, refrigerators, water coolers, and so on. In the case of the so-called heat pumping modules in the commercial devises, the separation between the heat absorption side (HAS) and the heat production one (HPS) are not so large, for example, within a few cm. The separation between the HAS and the HPS should be, however, more variable, so to say, from a few cm to hundreds of km, for more various applications, such as shown in Fig. 3(a), as a circuit system with the use of the Peltier effect. We call here the circuit system in Fig. 3(a) as "the electronic heat pumping system", in order to distinguish the present system from the conventional gaseous heat pumping system. We have done demonstrative experiments for the electronic heat pumping system, using two sets of π type Peltier elements with about 225 cm separations [cf. Fig.3 (a)]. Here, .the left and the right side sets of four π type Peltier elements are connected as n-type to n-type and p-type to p-type in sires. Under two conditions for the left side Peltier elements, we have measured the temperature T_4 on the right hand side Peltier elements. At first, the left side Peltier elements have been put in surrounding air without any external temperature controller. Secondly, the temperature T_1 on the left side Peltier elements is kept at 10 ℃ by additional heating with an external temperature controller. Experimental results are shown in Fig. 3(b), where the lower curve denotes the data of T_4 for the case without any external temperature controller and the upper one represents the data of T_4 for the case with the external temperature controller. It can be seen from Fig. 3(b) that when the value T_1 on the left side is kept at 10 ℃ by additional heating with the use of the external temperature controller, the value of T_4 becomes higher than the case without the external. temperature controller. This experimental result clearly show that the additional thermal energy is transported from the left side set to the right side one by the electronic heat pumping as shown by the upper curve. By subtracting values on the

lower curve from those on the higher one in Fig. 3(b), we obtain the increased temperature of ΔT_4 by the electronic heat pumping under the additional heating to keep $T_1 = 10$ ℃, as is shown in Fig. 3(c). We see from Fig. 3(c) that the transported thermal energy corresponding to ΔT_4 is almost proportional to the circuit current I_c. As a result, we have confirmed by our experiments that the long distance transportation of the injected thermal energy is realized through the electronic heat pumping, so that the more additional heating to the endothermal side of Peltier elements and the higher current in the circuit do yield the greater thermal energy transportation. Next, we have done another demonstrative experiments for the electronic heat pumping, using two set of five π type Peltier elements with about 225 cm separations, as shown in Fig.3 (d) similar to Fig.3 (a). Here, both of the two sets of five π type Peltier elements in Fig.3 (d) are entirely enclosed by multiple layers of thin aluminum sheets, in order to make thermal energy containers with low heat capacity. The two aluminum thermal energy containers are thermally insulated from surrounding air by thin papers including air inside them. When the current flows in the circuit of Fig.3 (d), the Joule heating takes place to raise the temperatures T_1 and T_4 of the two sets of π type Peltier elements. If the endothermal energy and the exothermal one were canceled out within one set of π type Peltier elements, then T_1 and T_4 would increase with the same values. However, if cancellation of the endothermal energy and the exothermal one did take place between the exothermal side and the endothermal one which are connected by highly electrical conductive long wires in Fig.3 (d), then T_1 would increase faster and higher than T_4 due to the electronic heat pumping mechanism. Figure 3 (e) shows the experimental data of the measured T_1 and T_4. We recognize from the data in Fig. 3 (e) that the net thermal energy by Joule heating at the T_4 side is definitely transported to the T_1 side, and therefore the cancellation of the endothermal energy and the exothermal one has realized within a fairly short time of a few min. through the connection by highly electrical conductive long wires between the exothermal side and the endothermal one.

It should be emphasized here that the long distance separation between the HAS and the HPS of the Peltier circuit systems does not change any physical mechanisms for the Peltier effects, i.e., the two phenomena of the exothermal process and the endothermal one do occur at the same instance. This is because that the additional electrical potential due to free electrons flowed in the conductor pushes surrounding every electrons to be shifted along the conductor to induce the current, and the traveling speed of the additional electrical potential must equal to the electrostatic potential wave or the electromagnetic one along the conductor until it's arrival at the other end. Because of these physical mechanisms, the induced thermal energies (so to say "positive thermal energy") at the exothermal side connected by highly electrical conductive long cables are cancelled out with the absorbed thermal energies (so to say "negative thermal energy") at the endothermal side of the present electronic heat pumping system in Fig.3(a).

In the steady state phase, the thermal energy absorption by the π type Peltier effect elements with the temperature T_4 in Figs. 2(a) or 3(a) is written by

$$q_{BAT4} = M\alpha_{BAT4}T_4 I_c \equiv V_{ST4} I_c , \tag{9}$$

where M is the number of the π type Peltier effect elements, and $V_{ST4} \equiv M\alpha_{ABT4}T_4$ is the output voltage by the Seebeck effect. The circuit and the power balance equations in the steady state for the circuit in Figs. 2(a) or 3(a) are written, respectively, as follows,

$$I_c\left(R_1 + R_c + R_2\right) - \left(V_{ST1T2} + V_{ST3T4}\right) = V_{ex} , \tag{10}$$

$$I_c^2\left(R_1 + R_c + R_2\right) - I_c\left(V_{ST1T2} + V_{ST3T4}\right) = I_c V_{ex} , \tag{11}$$

where R_1 and R_2 represent the contact resistances at the HAS and the HPS, respectively, and $V_{ST1T2} \equiv M(\alpha_{ABT1}T_1 - \alpha_{ABT2}T_2)$ and $V_{ST3T4} \equiv M(\alpha_{ABT3}T_3 - \alpha_{ABT4}T_4)$ are the output voltages by the pair of the Seebeck effect elements. Since the power balance between the thermal input and the thermal out put from the closed surroundings of the system by using the Peltier effect must be satisfied in the steady state phase because of the energy conservation law, the total endothermal energy and the total exothermal one in the circuit system must be completely cancelled out. We then obtain the power balance equations of the thermal energy by the Peltier effect for the electronic heat pumping system of Figs. 2(a) or 3(a) as follows;

$$M\alpha_{ABT1}T_1 I_c - M\alpha_{ABT2}T_2 I_c + M\alpha_{ABT3}T_3 I_c - M\alpha_{ABT4}T_4 I_c = 0 , \tag{12}$$

Substituting Eq.(12) into Eq.(11), we obtain the final power balance equation, as follows

$$I_c V_{ex} = I_c^2 \left(R_1 + R_c + R_2 \right). \qquad (13)$$

We clearly find from Eq.(13) that the externally applied electrical power is used only for the Joule heating in the total resistance of $(R_1 + R_C + R_2)$, and the transportation of the thermal energy takes place independently from the external electrical power. This feature of the electronic heat pumping systems shown in Fig. 2(a) is common in the main concept for the general heat pumping systems, and it can be considered to be a remarkable advantage for development of electronic devices by using the Peltier effect elements.

The physical mechanism by the electronic heat pumping (EHP) system in Fig. 2(a) is completely different from the gaseous one (GHP), where the GHP is based on the physical mechanism by the energy transfer between the gaseous thermal- and the external mechanical energies by the adiabatic compression and expansion of the circulating gases. This different physical mechanism between the EHP and the GHP leads to the followings: 1) The speed of the heat transport is the speed of the electromagnetic wave along the cable conductors in the EHP, while the speed of the heat transport in the GHP is the circulating speed of the working gas in the gas pipe, i.e., heat transport time is almost negligible in the EHP compared with that in GHP. 2) In the case of the EHP, there is no mechanically moving elements, and Eq. (8) tells us that the heat absorption (or the heat production) always takes place in the conductors as far as the condition of $\phi_B(T_1) > \phi_M(T_1) > \phi_A(T_1)$ is kept. In other words, the temperatures at A of the HAS and at B of the HPS could have extremely low and high values, respectively, depending on their circumferences. 3) The absorbed thermal energy at the HAS is equal to the transported thermal energy at the HPS, i.e., the conservation of the thermal energy absorbed at the HAS and produced at the HPS is automatically guaranteed in the EHP, as discussed at Eq.(13). 4) Since the HAS and the HPS are flexibly separated, for example, the HAS is used for refrigerators or air conditioners, and at the same time, the HPS can be used independently for heating devices such as heating water pots, and the HTS of the Seebeck effect circuit system shown later, which can be placed at an arbitrary distance.

It should be noted here that the electronic heat pumping system with the use of the Peltier effect shown at Fig. 2(a) and/or Fig. 3(a) plays as a compressor of the thermal energy density through the transport of the thermal energy from the HAS to the HPS, for example, the thermal energy in air with fairly low thermal energy density because of room temperature is absorbed at the HAS and is transported to the metal at the HPS with higher thermal energy density due to heated by the Peltier effect. This role of the compressing thermal energy density is same for the usual gaseous heat pumping. In other words, through the transportation of the thermal energy to the metal with a small heat capacitance at the HPS, the compression of the thermal energy density is realized to increase the temperature T_4 of the metal. This increased temperature can be used for the following Seebeck effect circuit system.

In the same way as the heat pumping circuit system by the Peltier effect, the Seebeck effect circuit system can be established with a large separation between the higher temperature T_1 side (HTS) and the lower temperature T_4 one (LTS), as shown in Fig. 4-(a). Here, the labels A and B represent the same materials as was shown in Fig. 2 (a). The physical quantity of V_{out} is the out put voltage induced in the Seebeck effect circuit system, and R_c the total electrical resistance of the cables connecting the both sides of the HTS and LTS in Fig. 4-(a). We recognize that in the Seebeck effect circuit system, the thermal energy is directly converted to the electrical potential energy, as far as the condition of $T_1 > T_4$ is kept in the open system. In the same way as the circuit equation of Eq. (10) for the circuit in Figs. 2(a) or 3(a), the circuit equation of the Seebeck effect system without V_{oex} in Fig.4(a), which has no external electrical power and no current in the circuit, is written as follows;

$$V_{out} - [M(\alpha_{ABT1} T_1 - \alpha_{ABT2} T_2) + M(\alpha_{ABT3} T_3 - \alpha_{ABT4} T_4)] = 0. \qquad (14)$$

When we set $T_2 \fallingdotseq T_3$, the third term of the left hand side of Eq.(14) vanishes. Since the relative Seebeck coefficient has usually a weak dependence on the temperature, we can put as $\alpha_{ABT4} = \alpha_{ABT1}$ and therefore we obtain the following equation for the output voltage V_{out} by the Seebeck effect;

$$V_{out} = M \alpha_{ABT4} (T_1 - T_4). \qquad (15)$$

We find from Eq. (15) that V_{out} by the Seebeck effect is proportional to the temperature difference $\Delta T = T_1 - T_4$. We

have done demonstrative experiments using two sets of Peltie elements with $M = 30$ and about 30 cm separation between the two sets, as shown in Fig.4 (b), where .the left and the right hand side of fifteen elements are connected as n-type to n-type and p-type to p-type in sires. Figure 4 (c) shows experimental dependence of V_{out} by the Seebeck effect on the externally applied variable of $\Delta T = T_1 - T_4$ in Fig.4 (b). It is seen from Fig. 4 (c) that V_{out} increases almost proportional to ΔT up to around 250.0 mV at $\Delta T \fallingdotseq 100$ ℃, as is expected by the analytical equation Eq. (15). If we increase the number of Peltie elements, for examples, 20 times of fifteen Peltie elements, i.e., 600 Peltie elements for Fig.4 (b), then the data of Fig. 4 (c) give us an estimated $V_{out.} \fallingdotseq 5.00$ V for $\Delta T \fallingdotseq 100$ ℃. This estimated value of $V_{out.}$ is enough to drive the heat pumping Peltier effect circuit system with around 600 Peltier elements shown as Fig. 3 (b) without any external electrical power. This experimental result indicates that the system proposed in Fig. 4 (a) has a good direct energy transfer from the thermal to the electrical potential energies with fairly long separation, and gives us freedom to establish easily the electrical power plants with the various separation distances between the HTS area and the LTS one. We do not need the fossil fuels such as coals, oils, and also the nuclear fission, all of them leave environmental pollutions.

It should be emphasized here again that the long distance separation between the HAS and the HPS of the Peltier circuit system or the HTS and the LTS of the Seebeck circuit one does not change any physical mechanisms for the both effects.

II-3. Permanent auto-working direct heat energy conversion systems from environmental thermal energies to the electrical – and/or chemical potential energy resources

We present here innovative permanent auto-working direct energy converting systems (PA-DEC systems) from the environmental thermal to the electrical and further the chemical (TEC) potential energy resources. Hereafter we abbreviate this kind of systems as the PA-TEC-DEC systems.

(PA-1) At first, we add the Seebeck thermoelectric circuit system to the heat pumping system by the Peltier effect circuit of Fig. 2, as shown in Fig. 5(a). Here, Fig. 5(a) is the PA-TE-DEC system, where the Seebeck effect circuit system is simply added on Fig. 2(a). In Fig. 5(a), the part of the thermal energy transportation is denoted by the mark <1>, and the part of the DEC with the positive feedback system by the Seebeck effect output voltage is shown by the mark <2>. The subscript S represents elements concerning with the Seebeck effect. Operating sequence of this PA-TE-DEC systems shown in Fig. 5(a) is as follows: 1) We close the switch 1 and open the switch 2. By this state of circuits, the thermal energy is transported from the HAS to the HPS at the mark <1> to make the temperature T_2 higher and higher. In order to raise the temperature T_3 at the HTS of the Seebeck effect circuit system, the HTS is contacted to the HPS of the Peltier effect circuit system with the use of the thermally conductive insulator, such as the silicon oil. 2) After the value of $V_{out.}$ have become high enough to drive the heat pumping circuit by the positive feedback driving voltage, we close the switch 2 and open the switch 1, and resultantly the PA-TE-DEC system is established to work without the first external battery.

(PA-2) Next, we show the operating sequence of the improved PA-TE-DEC systems shown in Fig. 5(b): 1) We close the switch 1. 2) Heat the HTS at the mark <2> with the use of some external heater such as fire of woods or a portable heater, so that the temperature T_3 becomes higher and higher. 3) After the value of $V_{out.}$ have become high enough to drive the heat pumping circuit by the positive feedback driving voltage, we close the switch 2 and open the switch 1, and the PA-TE-DEC system is established resultantly to work with lesser initial external input energy. The current, I_C, continues to flow by the positive feedback circuit, as far as we keep the condition of $T_3 > T_4$.

The physical reason why we can realize this type of the PA-TE-DEC system is as follows: (1) In the heat pumping circuit by the Peltier effect in Figs. 5(a) and 5(b), the environmental thermal energy absorbed from circumferential material at the left side is continuously transported from the left hand side to the right hand one to be condensed thermal energy density, as far as the condition T_3 at the HTS > T_4 at the LTS is kept to yield high enough positive feedback $V_{out.}$ by the Seebeck effect circuit. (2) When electrical current flows in the Seebeck effect circuit, this circuit works as the heat pumping circuit by the Peltier effect to absorb the thermal energy at the HTS and produce the thermal energy at the LTS. (3) Due to the combination of (1) and (2), the thermal energy continuously flows from the regions of T_1 to T_2, T_3, and finally to T_4 in this total system. Since this PA-TE-DEC system is the thermally open system, the entropy law of thermodynamics in the closed system is not available. We know that the earth itself is one of the open systems, and the thermal energy circulation supports all lives on the earth and also the weather changes every day. Here, the thermal energy changes always its type, such as the electrical energy, the chemical one, the

hydrodynamic one, and so on, and human uses some part of them as an available energy resources.

Now, we add further a resolving water part as a load for the electrical out put on the system of Fig. 5(a), as shown in Fig. 6(a). Here, Fig. 6(a) is the system, where the resolving water part is added on Fig. 5(a), and Fig. 6(b) is that, where the resolving water part is added on Fig. 5(b).

We propose the simplest PA-TEC-DEC system, which has only the Seebeck effect circuit system and the resolving water part, as shown in Fig. 7. We can see from Figs. 6 and 7 that the electrical potential energy at the Seebeck effect parts is converted to the chemical potential energy as the hydrogen gas and the oxygen one, which are easily compressible and conveyable depending on the porpoise of their usages.

When we consider the steady state of the PA-TEC-DEC systems shown at Figs. 6(a) and 6(b), we can write the circuit equation and the power balance one, respectively, as follows;

$$M(\alpha_{ABT1}T_1 - \alpha_{ABT2}T_2) + N(\alpha_{ABT3}\lambda T_3 - \alpha_{ABT4}T_4) = I_L\left(R_{c1} + R_{c2} + R_L\right), \tag{16}$$

$$M(\alpha_{ABT1}T_1 - \alpha_{ABT2}T_2)I_L + N(\alpha_{ABT3}\lambda T_3 - \alpha_{ABT4}T_4)I_L = I_L{}^2\left(R_{c1} + R_{c2} + R_L\right), \tag{17}$$

where R_{c1}, R_{c2} and R_L represent respectively the total circuit resistances of the heat pumping Peltier effect circuit, the Seebeck effect circuit, and the load circuit including the effective water resolving resistance, and λ ($\leqq 1.0$) denotes the coefficient of the thermal energy transfer from the part of T_2 to that of T_3, for example, no thermal loss correspond to $\lambda = 1.0$. Since the left hand side of Eq. (17) indicates the net absorbed power of the external thermal energy into the circuit by the Peltier effect, this equation shows that the energy conservation law is exactly satisfied in a simple form where the net absorbed thermal power is directly transferred to the electrical power of the effective Joule heating in the circuit. We can see from Eq. (17) that when $M = 0$, corresponding to the case of Fig. 7, then the difference of the thermal flow power between the absorbed thermal energy at the HTS and the exhorted thermal energy at the LTS is used for the electrical power output (the right hand side term of Eq. (17)). The first term of the left hand side of Eq. (16) by the heat pumping circuit acts as the effective resistance against the output voltage by the Seebeck effect of the second term. When we make ideal thermal insulation around the parts of T_2 and T_3, i.e., $\lambda = 1.0$, the temperature T_2 becomes to be equal to T_3. Taking account of the weak dependence of the relative Seebeck coefficient on the temperature, we can rewrite Eq. (16) in a simpler from as follows;

$$\alpha_{ABT3}[N(T_3 - T_4) - M(T_3 - T_1)] = I_L\left(R_{c1} + R_{c2} + R_L\right). \tag{18}$$

Since $I_L > 0$ is the necessary and sufficient condition for the realization of the PA-TES-DEC system, we obtain the following condition from Eq. (17) in order to establish the present PA-TES-DEC system.

$$N(T_3 - T_4) > M(T_3 - T_1), \tag{19}$$

We find the following interesting cases from Eq. (19): 1) The $M = 0$ case is the case of Fig. 7, and the condition of $T_3 > T_4$ is easily satisfied to realize the PA-TES-DEC system. 2) When the heat source areas with fairly high temperature, such as the Sahara Desert, volcano area, deep high temperature regions inside the earth, and so on, are very far from the place where we need available energy resources, then using the heat pumping system in Fig. 6(b), we can make the steady state with $T_3 = T_2 = T_1$ and realize the PA-TES-DEC system which satisfies the condition of Eq. (19). In this case, the thermal energy transfer by the heat pumping system becomes very useful and the use of the high temperature super conductors for the long cables will be inevitable for the high transformation efficiency from the thermal energy to the electrical or the chemical energies, corresponding to the ratio $R_L/(R_{c1} + R_{c2} + R_L)$ in Eq. (17).

Using hot water flow to keep $T_2 = 76$ °C and a cooling fan to keep $T_3 = 29$ °C, we had also done a preliminary experiment on the resolving water system. This experiment corresponds to the case where we picked up two parts of <2> and <3> in Fig. 6(a). Using this experimental system with $\Delta T = T_2 - T_3 = 37$ °C, we had obtained H_2 gas of about 40.0 cc and O_2 gas of about 20.0 cc at the pressure of the atmosphere on the earth level after 30 min. These experimental results indicate that using the thermal energy input, we obtain the chemical energy power of about 15.6 mW and the chemical energy of about 7.81 mWH.

If we use more Peltier elements, for example 1000 set of the π type Peltier elements, we can drive motor by burning the

hydrogen gas exhorting just water, or by using the hydrogen fuel battery. Instead of the resolving water system, we can directly put the storage battery at the part of <3>, which is also conveyable and the chemical potential energy storage system itself, being considered usually the electrical energy storage system for the electrical power supply.

We may find that the present PA-TEC-DEC system with the use of the continuous thermal energy flow system can be used for new plants of electrical power and also hydrogen gas resources without environmental pollutions. Since the solar battery reflects over 60 % of the solar energy, being lowered its efficiency of the energy conversion, if we use suitable black materials in addition to solar battery panels, then all energy of the solar light can be absorbed into the combined black materials to use for the present PA-TEC-DEC system and to yield high energy conversion system with fairly high efficiency.

III. CONCLUDING REMARKS

We have shown that with the use of the fusion output and/or environmental thermal energy, innovative open systems for permanent auto-working (PA) direct energy converting (DEC) from the thermal to the electrical (TE) and further to the chemical potential (TEC) energies, abbreviated as PA-TEC-DEC systems, can be used for new auto-working electrical power plants and the plants of the compressible and conveyable hydrogen gas resources. We have clarified theoretically the physical mechanisms of the Peltier effect and the Zeebeck one in Section II-1 [cf. from Eq.(1) to Eq.(8)]. We have also clarified analytically that the externally applied electrical power is used only for the Joule heating in the total resistance of the circuit, and the transportation of the thermal energy by the electronic heat pumping (EHP) system takes place independently from the used power of the external electrical source in Section II-2 [cf. from Eq.(9) to Eq.(13)]. We have noted four favorable features from 1) to 4) of the EHP system compared with the gaseous heat pumping (GHP) after Fig. 2(a), and have shown that the EHP system can be used for various porpoises.

We have demonstrated by experiments shown at Figs. 2(b) to 2(d), and Figs. 3(a) to 3(e) that the EHP system with long separating cables works well as expected. We have confirmed by our experiments that the long distance transportation of the injected thermal energy is realized through the EHP system, so that the more additional heating to the endothermal side of Peltier elements and the higher current in the circuit do yield the greater thermal energy transportation. Since the HAS and the HPS are flexibly separated, the HAS is used for devices such as refrigerators, air conditioners, and all cooling systems. At the same time, the HPS can be used independently for heating devices such as the heater for the TE-DEC circuit systems to generate electrical power, heating water pots and all heating water pool systems, which can be placed at any arbitrary distances. We have also clarified that the long distance separation between the HAS and the HPS in the Peltier effect circuit system and between the HTS and the LTS in the Seebeck effect circuit system does never change any physical mechanisms for the both effects

We have demonstrated experimentally at Figs. 4(a), 4(b), and 4(c) that the proposed Seebeck effect circuit system has a good direct energy converter from the thermal to the electrical potential energies with fairly long separation between HTS area and the LTS one. We have clarified at Fig. 4(c) that with the use of two sets of 30 Peltie elements with about 30 cm separation between the two sets, the output voltage by the Seebeck effect increases almost proportional to ΔT up to around 250.0 mV at $\Delta T \fallingdotseq 100$ ℃, as is expected by the analytical equation Eq. (15). This experimental result gives us freedom to establish easily the electrical power plants with the various separation distances between the HTS area and the LTS one, without using such as oils, nuclear fissions, i.e., without environmental pollutions.

We have proposed at Figs. 5(a), 5(b), 6(a), 6(b), and 7 in Section II-3 that the PA-TEC-DEC system with the use of the continuous thermal energy flow system can be used for new plants of electrical power and also hydrogen gas resources without environmental pollution. We have analytically proved by Eq. (17) that the energy conservation law is exactly satisfied in a simple form where the net absorbed thermal power is directly transferred to the electrical power of the effective Joule heating in the circuit system. We have clarified analytically that the necessary and sufficient condition for the realization of the proposed PA-TEC-DEC system can be expressed in a simple form of Eq. (19) deduced from the circuit equation and the power balance one (cf. Eqs. (16) – (19)). Using Eq. (19), we have shown interesting cases to establish real PA-TEC-DEC systems, one of which is the case where the heat source areas with fairly high temperature are very far from the place where we need available energy resources. We have also discussed about the high transformation efficiency from the thermal energy to the electrical or the chemical energies, corresponding to the ratio $R_L/(R_{c1}+R_{c2}+R_L)$ in Eq. (17), for example, if we use the high

temperature supper conductors for the connecting cables in the PA-TEC-DEC systems, then this transformation efficiency could become very close to unity.

It is important to emphasize again that since and the entropy law established in the closed system is not applicable for the proposed open systems, the PA-TEC-DEC systems do work physically well because of the feature of their open systems. We may expect easily that if the present innovated systems would be used world widely, the green house effect by the CO_2 gas should be decreased

ACKNOWLEDGRMENTS

The authors appreciate greatly Messrs. Y. Kato, and D. Okada, and Drs. K. Itoh, and N. Iwasawa for their valuable discussion and help on experiments. Two of the authors (Y. K. and T. T.) would like to express their appreciation to Dr. Y. Tomita, NIFS, for his advise on the direct energy conversion systems for the fusion energy plant. They would like to thank Mr. K. Goto, Director of Environmental System Business Unit, Mr. K. Tamura, Director, and Mr. S. Sato, Senior Manager, Central Research Laboratory for Eco-field, Meidensha corporation, Japan, for their collaborating discussion and their financial support.

References

[1] Kondoh, Y., Stable Equilibrium Configuration of a Reversed Field Pinch with Partially Relaxed State Condition, *Nucl. Fusion* 21, 1607-1613 (1985).

[2] Kondoh, Y., An Energy Principle for Axisymmetric Toroidal Plasmas *J. Phys. Soc. Jpn.* 54. 1813-1822 (1985).

[3] Kondoh, Y., Yamagishi, T & M. S. Chu, Stability Conditions for Pertubations with Singularity Derived from Energy Principle, *Nucl. Fusion* 27 . 1473-1473 (1987) .

[4] Kondoh, Y., Reminimization of Energy Integral and Transition Point of Mode for Relaxed States of Nonideal MHD Plasma, *J. Phys. Soc. Jpn.* 58. 489-503 (1989).

[5] Kondoh, Y., Eigenfunction for dissipative dynamic operators and the attractor of the dissipative structure, *Phys. Rev.* E 48. 2975-2979 (1993) .

[6] Kondoh, Y., Attractors of Dissipative Structure in Three Dissipative Fluids, *Phys. Rev.* E 49. 5546-5555 (1993) .

[7] Kondoh, Y. & Van Dam, J. W. Self-organization of solitons for the Korteweg-de Vries equation, *Phys. Rev.* E 52, 1721-1725 (1995) .

[8] Kondoh, Y., Yoshizawa, M., Nakano, A & Yabe, T., Self-organization of two-dimensional incompressible viscous flow in a friction-free box, *Phys. Rev.* E 54, 3017-3020 (1996) .

[9] Kondoh, Y., Yamaguchi, M.& Yokozuka, K., *J. Phys. Soc. Jpn.* 66 (1997) 288.

[10] Kondoh, Y., Kondo, M., Shimoda, K., Takahashi, T., and Itoh; K., Innovative direct energy conversion systems using electronic adiabatic processes of electron fluid in solid conductors : new plants of electrical power and hydrogen gas resources without environmental pollutions, *Research report of National Institute for Fusion Science, Japan*, NIFS-TECH-11, July 2001.

[11] Ioffe, A. F., Semicoductor Thermoelements and Thermoelectric Cooling, *London, Infosearch Ltd.* (1956) .

[12] Heikes, R. R. & Ure, R. W. Jr, Thermoelectricity: Science and Engineering, *New York, Intescienece Publishers* (1960).

[13] Nussbaum, A., Semiconductor Device Physics, *Prentice-Hall, Inc.*(1962).

[14] Rowe, D. M., & Bhandari, C. M., Modern Thermoelectrics, *London, Holt, Rinehart and Winston* (1983).

[15] Rowe, D. M. & Bhandari, C. M., Modern Thermoelectrics, *London, Holt, Rinehart and Winston* (1983).

[16] Ogawa, Y., Ueda, K., & Sugawara, H., Magnetic effect on Peltier supper cooling system, *J. Advanced Science* 8, 137-142 (1992).

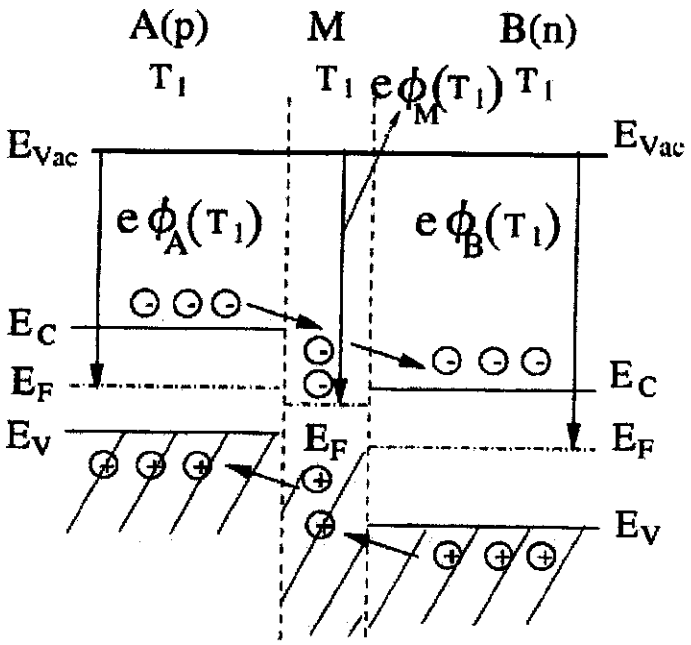

Fig.1. Schematic drawing of energy band diagram around two contact surfaces between A(p) and M(metal), between M and B(n). Here, the Fermi energy levels E_F in A, M and B have shown like a staircase due to the externally applied electric field, the potentials $\phi_A(T_1)$, $\phi_M(T_1)$, $\phi_B(T_1)$ are measured from vacuum level E_{VAC} to the Fermi level E_F, T_1 is the temperature arround the two semiconductors of A and B and the copper metal, which have the feature of $\phi_A(T_1) < \phi_M(T_1) < \phi_B(T_1)$.

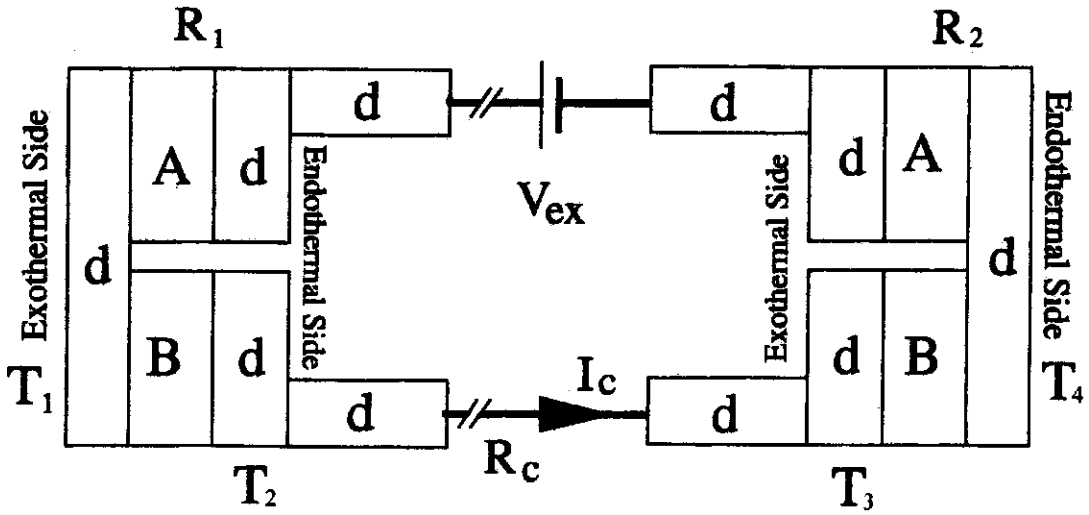

Fig.2(a) A circuit with two sets of π type Peltier effect elements with arbitrary separations between the two sets.

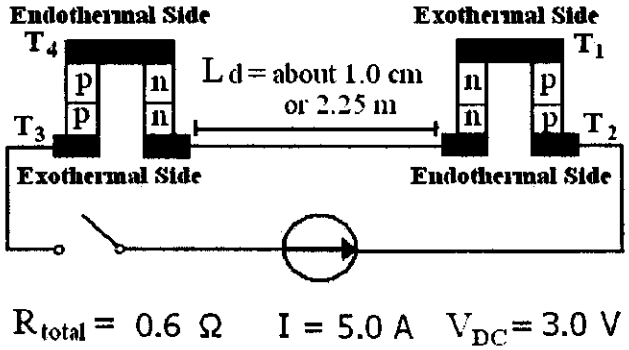

Fig.2(b) Demonstrative experimental system, using two set of four or five π type Peltier elements with two separations of about 1 cm and 225 cm.

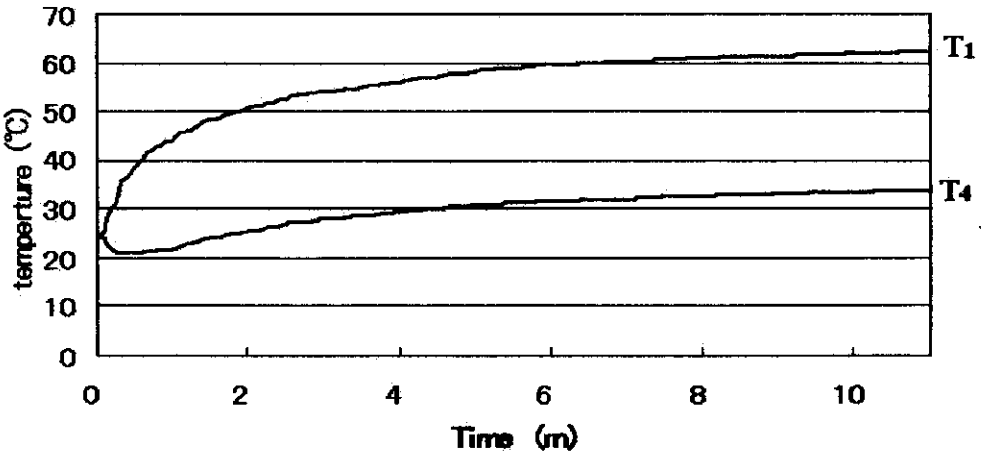

Fig.2(c) Experimental data for the case of about 1 cm separation between the two set of of four π type Peltier elements in Fig. 2 (b).

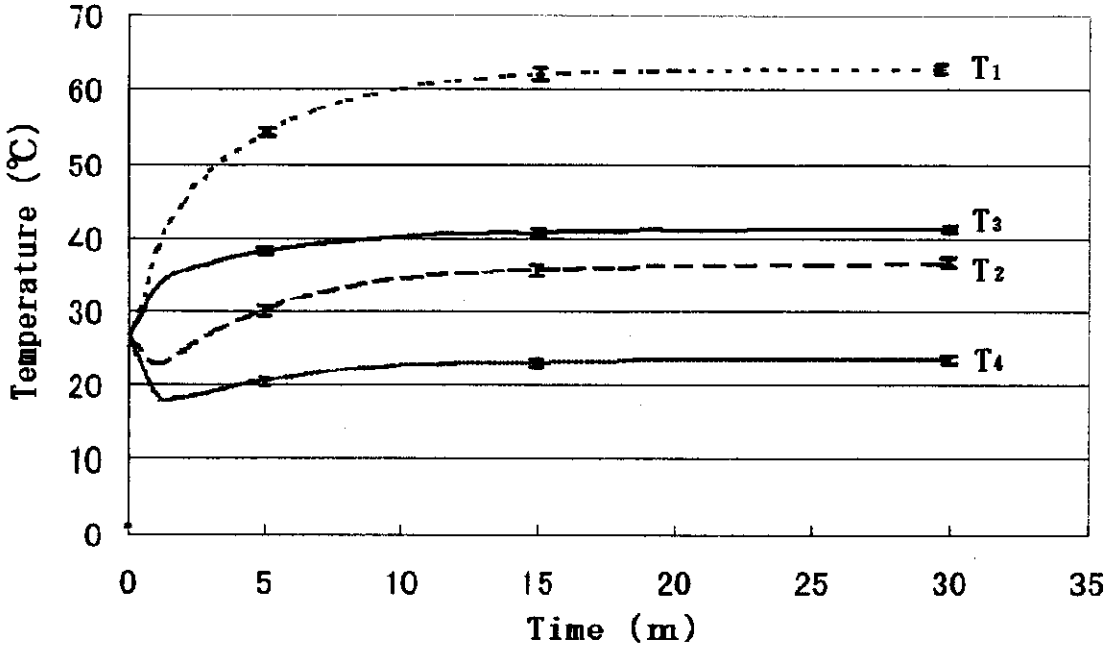

Fig.2(d) Experimental data for the case of about 225 cm separation between the two set of five π type Peltier elements in Fig. 2 (b).

Fig. 2. Peltier effect circuit systems.

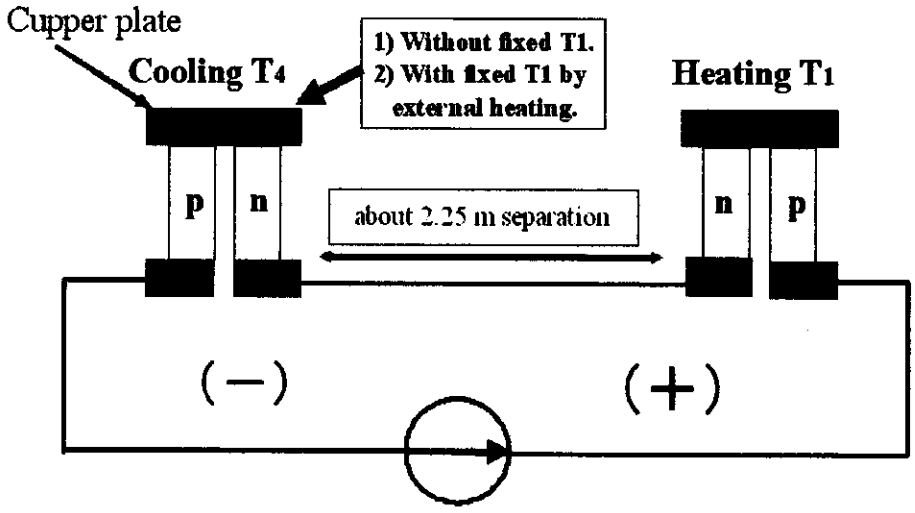

Constant current source with 5.0 A and 2.5 V

Fig.3(a) Demonstrative experimental circuit for the EHP, using two set of four π type Peltier elements with about 225 cm separation.

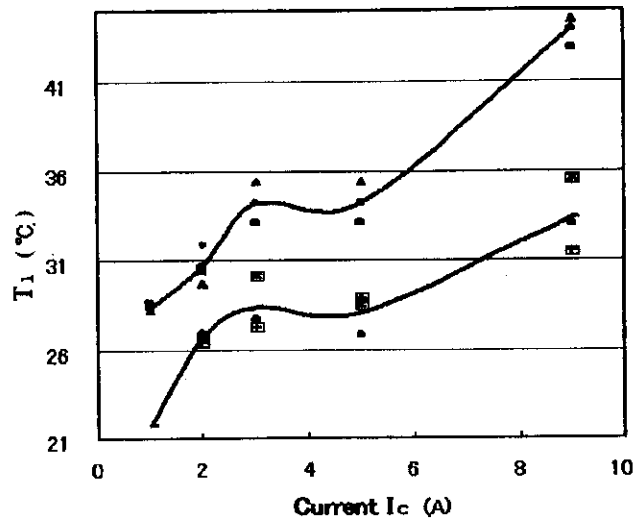

Fig.3(b) Experimental results, where the lower curve denotes the data of T_1 for the case without any external temperature controller and the upper one represents T_1 for the case with the external temperature controller to keep $T_4 = 10$ ℃.

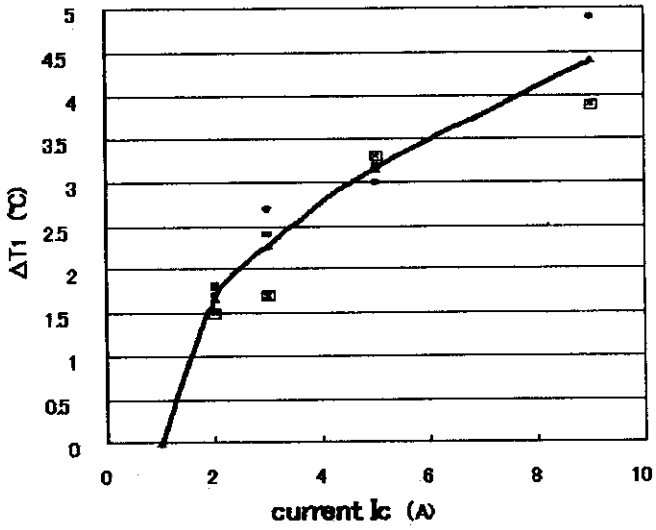

Fig.3(c) Increased temperature of ΔT_1 by the EHP under the additional heating to keep $T_4 = 10$ ℃ obtained by subtracting the lower curve from the higher one in Fig. 3(b).

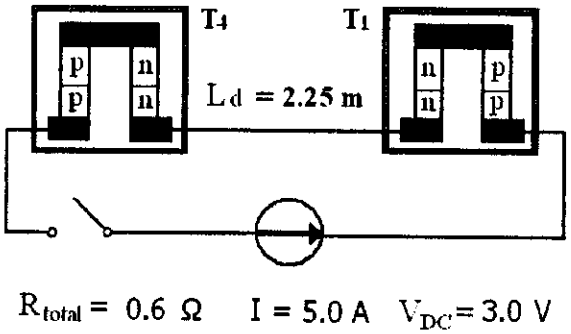

Fig.3(d) Another demonstrative experimental circuit for the EHP, using two set of five π type Peltier elements with about 225 cm separation. Both of the two set of five π type Peltier elements are entirely enclosed by thin aluminum sheets in order to make thermal energy containers with low heat capacity.

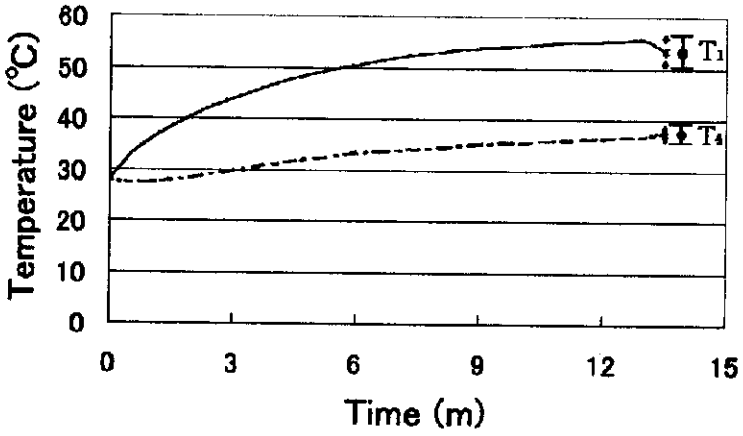

Fig.3(e) Experimental data of the measured T_1 and T_4 in Fig. 3(d).

Fig. 3. Electronic heat pumping (EHP) systems by the Peltier effect with arbitrary separation between the heat absorption side (HAS) and the heat production one (HPS).

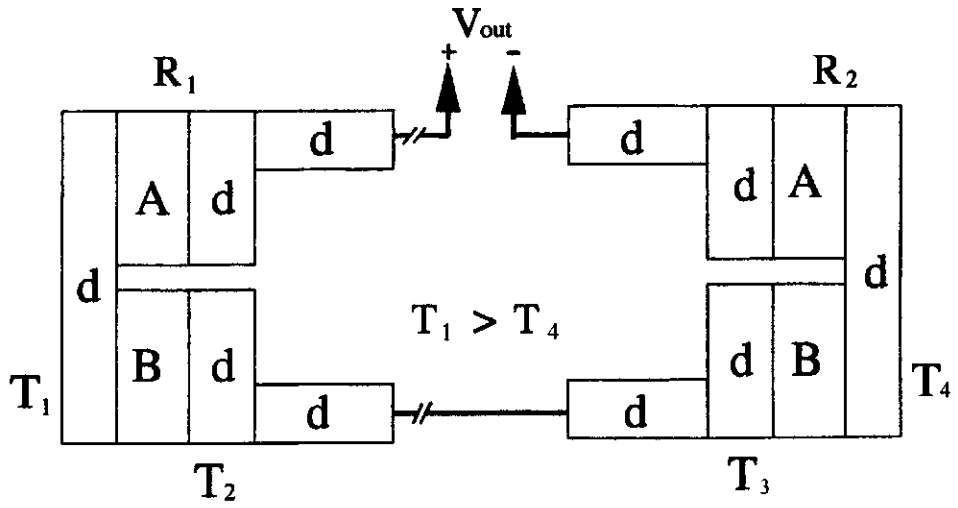

Fig.4(a) A circuit with two sets of π type Seebeck (Peltier) effect elements with arbitrary separations between the two sets.

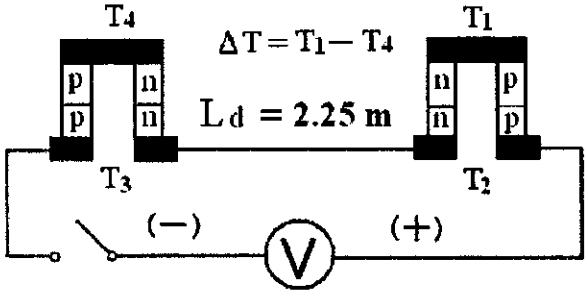

Fig.4(b) Demonstrative experimental circuit system by Seebeck effect, using two set of 30π type Peltier elements with about 30 cm separation.

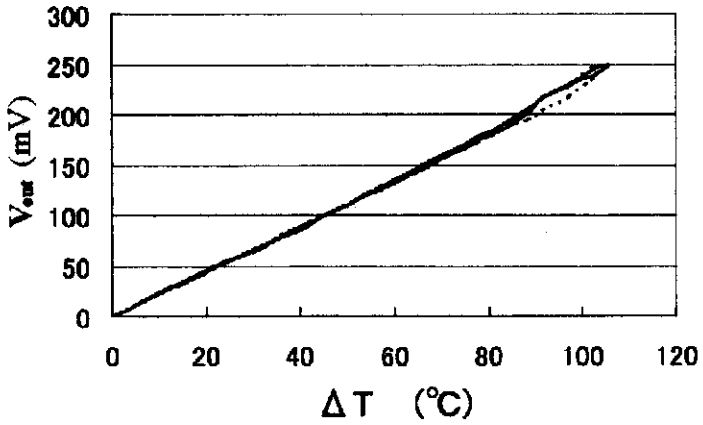

Fig.4(c) Experimental dependence of the out put voltage V_{out} by the Seebeck effect on the externally applied variable of $\Delta T = T_1 - T_4$

Fig. 4. Seebeck effect circuit systems.

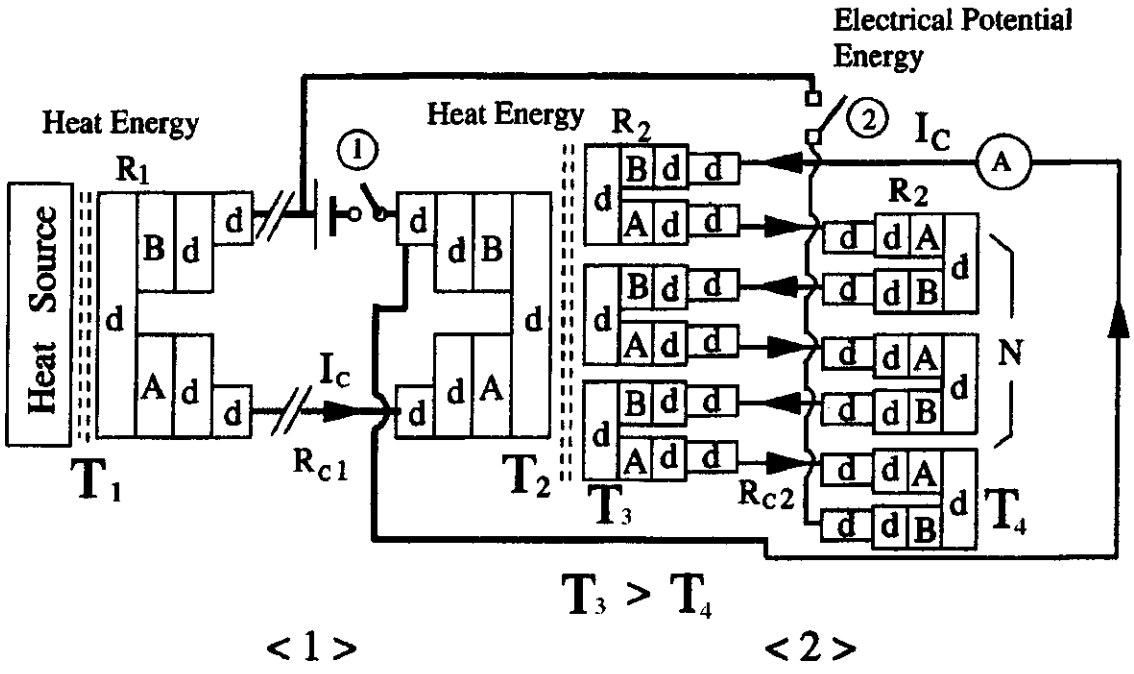

Fig.5(a) Feedback system with the use of initial external electrical power.

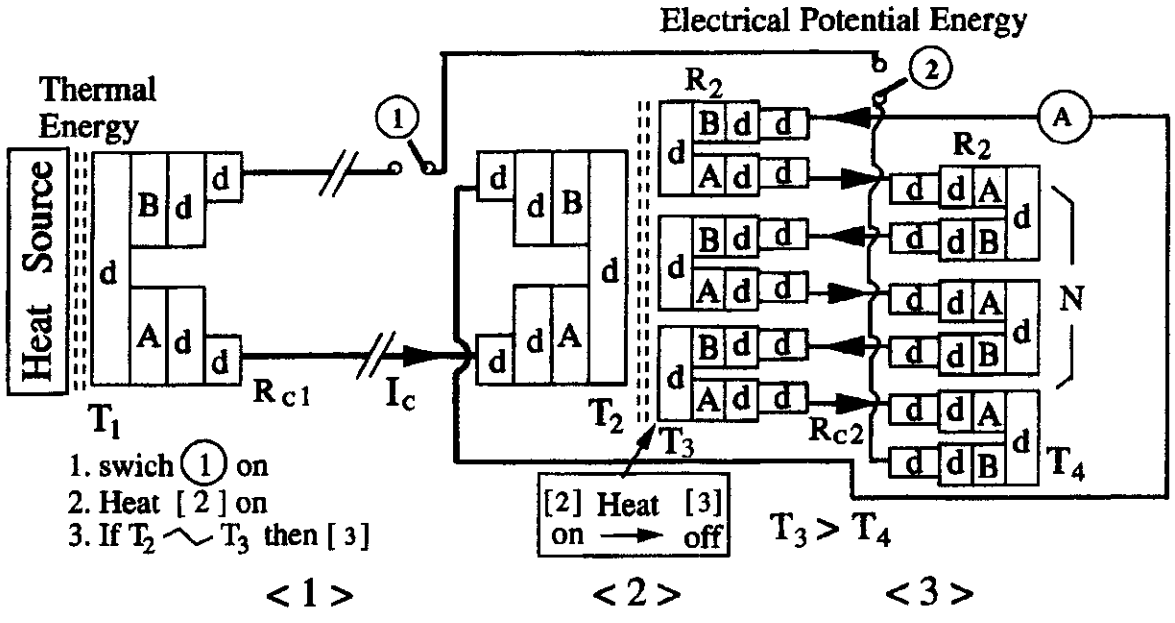

Fig.5(b) Feedback system without initial electrical power.

Fig.5. Permanent auto-working (PA) systems of the EHP added with the Seebeck thermoelectric circuit for a positive feedback.

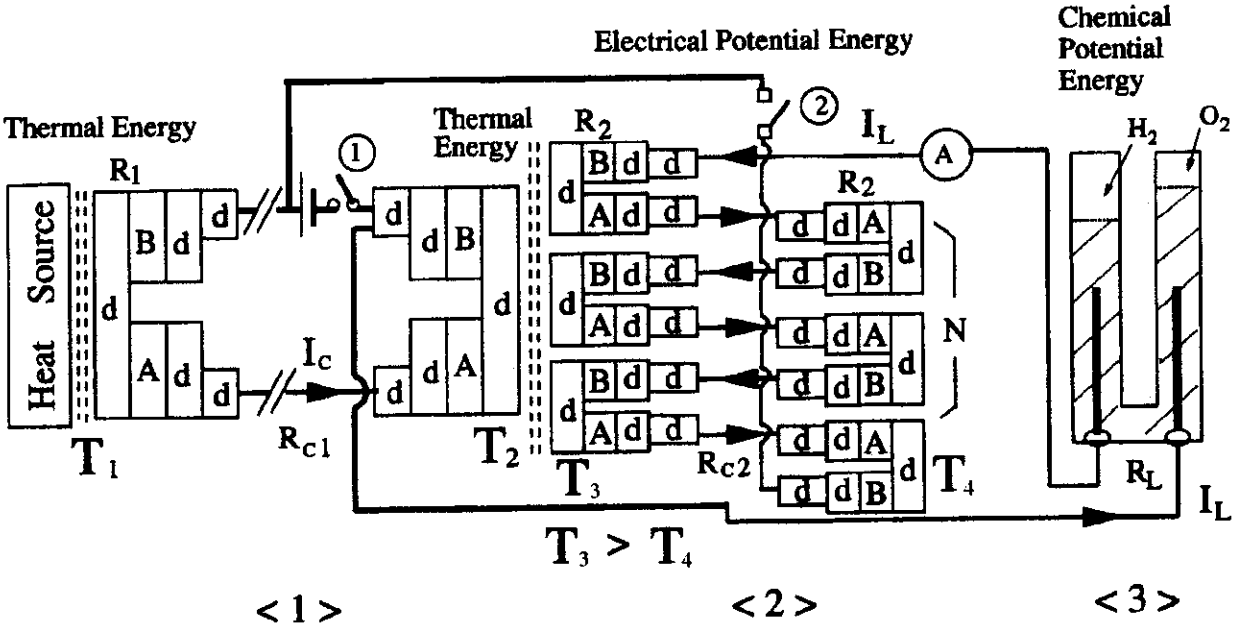

Fig.6(a) The PA system with initial external electrical power.

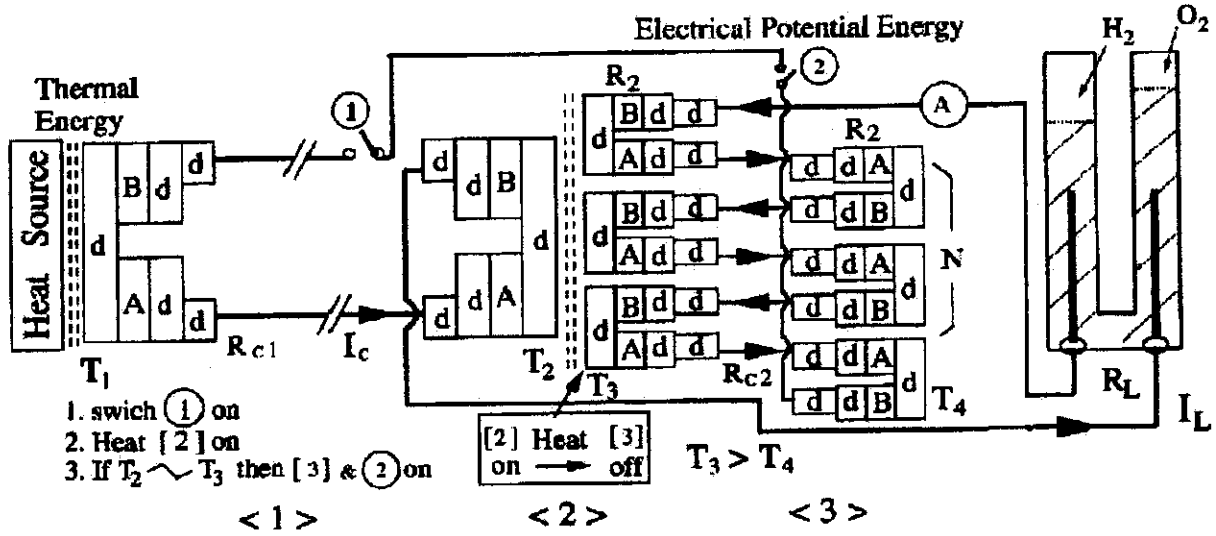

Fig.6(b) The PA system without initial electrical power.

Fig.6. .The PA systems combining the EHP by the Peltier effect, the feedback circuit by the Seebeck effect, and the chemical energy production part by resolving water.

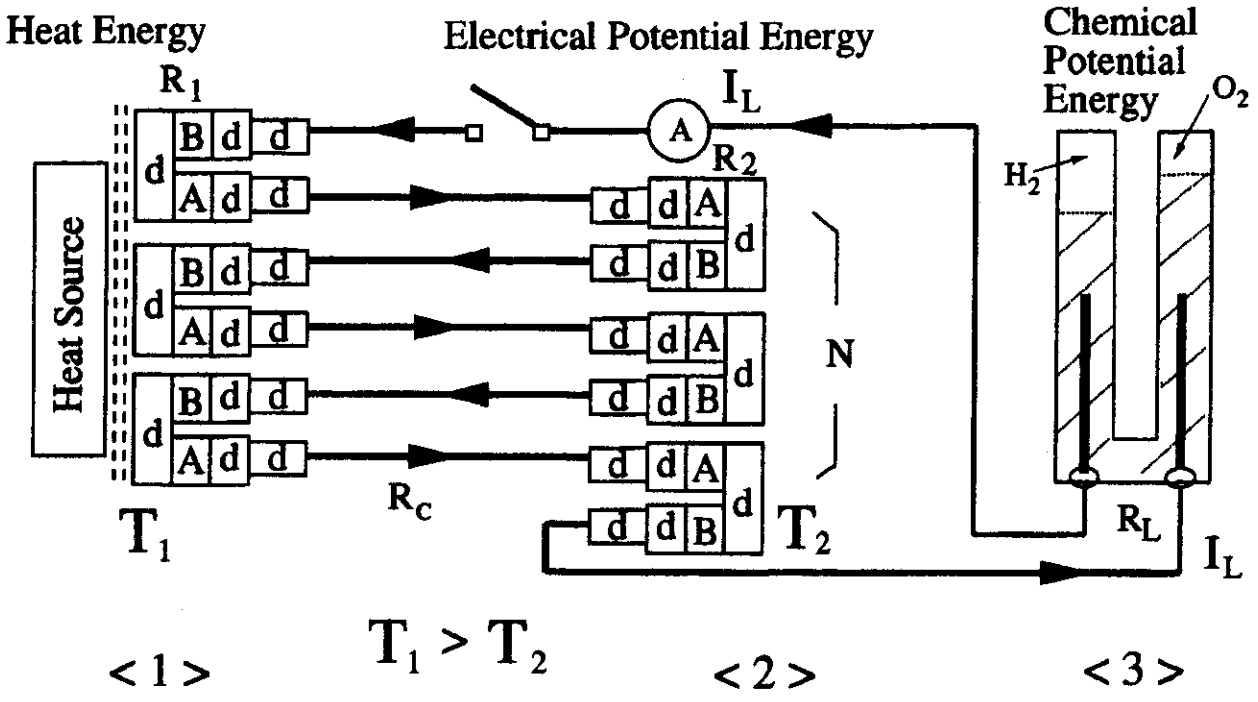

Fig. 7 The simplest PA-TEC-DEC system which has only the Seebeck effect components and the resolving water part.

Recent Issues of NIFS Series

NIFS-757 H. Ohtani, R. Horiuchi and T. Sato
Profile Relaxation and Tilt Instability in a Field-Reversed Configuration
Oct. 2002 (TH/P2-11)

NIFS-758 K. Toi, S. Ohdachi, S. Yamamotoa, N. Nakajima, S. Sakakibara, K.Y. Watanabe, S. Inagaki, Y. Nagayama, Y. Narushima, H. Yamada, K. Narihara, S. Morita, T. Akiyamab, N. Ashikawa, X. Dinge, M. Emoto, H. Funaba, M. Goto, K. Ida, H. Idei, T. Ido, K. Ikeda, S. Imagawa, M. Isobe, K. Itoh, O. Kaneko, K. Kawahata, T. Kobuchi, A. Komori, S. Kubo, R. Kumazawa, J. Lid, Y. Liang, S. Masuzaki, T. Mito, J. Miyazawa, T. Morisaki, S. Murakami, S. Muto, T. Mutoh, K. Nagaoka, Y. Nakamura, H. Nakanishi, K. Nishimura, A. Nishizawa, N. Noda, T. Notakea, K. Ohkubo, I. Ohtake, N. Ohyabu, Y. Oka, S. Okamura, T. Ozaki, B.J. Peterson, A. Sagara, T. Saidae, K. Saito, R. Sakamoto, M. Sasao, K. Sato, M. Sato, T. Satow, T. Seki, T. Shimozuma, M. Shoji, S. Sudo, M.Y. Tanaka, N. Tamurae, K. Tanaka, K. Tsumori, T. Uda, T. Watari, A. Wellerf, Y. Xu, I. Yamada, M. Yokoyama, S. Yoshimura, Y. Yoshimura, K. Yamazaki, K. Matsuoka, O. Motojima, Y. Hamada, M. Fujiwara
MHD Instabilities and Their Effects on Plasma Confinement in the Large Helical Device Plasmas
Oct. 2002 (EX/S3-2)

NIFS-759 S. Kubo, T. Shimozuma, H. Idei, Y. Yoshimura, T. Notake, M. Sato, K. Ohkubo, T. Watari,K. Narihara, I. Yamada, S. Inagaki, Y. Nagayama, S. Murakami, S. Muto,Y. Takeiri, M. Yokoyama, N. Ohyabu, K. Ida, K. Kawahata, O. Kaneko, A. Komori, T. Mutoh, Y. Nakamura, H. Yamada, T. Akiyama, N. Ashikawa, M. Emoto, H. Funaba, P. Goncharov M. Goto, K. Ikeda, M. Isobe, H. Kawazome, K. Khlopenkov, T. Kobuchi, A. Kostrioukov, R. Kumazawa, Y. Liang, S. Masuzaki, T. Minami, J. Miyazawa, T. Morisaki, S. Morita, H. Nakanishi, Y. Narushima, K. Nishimura, N. Noda, H. Nozato, S. Ohdachi, Y. Oka, M. Osakabe, T. Ozaki, B. J. Peterson, A. Sagara, T. Saida, K. Saito, S. Sakakibara, R. Sakamoto, M. Sasao, K. Sato, T. Seki, M. Shoji, H. Suzuki, N. Takeuchi, N. Tamura, K. Tanaka, K. Toi, T. Tokuzawa, Y. Torii, K. Tsumori, K. Y. Watanabe, Y. Xu, S. Yamamoto, T. Yamamoto, M. Yoshinuma, K. Itoh, T. Satow, S. Sudo, T. Uda, K. Yamazaki, K. Matsuoka, O. Motojima, Y. Hamada and M. Fujiwara
Transport Barrier Formation by Application of Localized ECH in the LHD
Oct. 2002 (EX/C4-5Rb)

NIFS-760 T. Hayashi, N. Mizuguchi, H. Miura, R. Kanno, N. Nakajima and M. Okamoto
Nonlinear MHD Simulations of Spherical Tokamak and Helical Plasmas
Oct. 2002 (TH/6-3)

NIFS-761 K. Yamazaki, S. Imagawa, T. Muroga, A. Sagara, S. Okamura
System Assessment of Helical Reactors in Comparison with Tokamaks
Oct. 2002 (FT/P1-20)

NIFS-762 S. Okamura, K. Matsuoka, S. Nishimura, M. Isobe, C. Suzuki, A. Shimizu, K. Ida, A. Fujisawa, S. Murakami, M. Yokoyama, K. Itoh, T. Hayashi, N. Nakajima, H. Sugama, M. Wakatani, Y. Nakamura, W. Anthony Cooper
Physics Design of Quasi-Axisymmetric Stellarator CHS-qa
Oct. 2002 (IC/P-07)

NIFS-763 Lj. Nikolic, M.M. Skoric, S. Ishiguro and T. Sato
On Stimulated Scattering of Laser Light in Inertial Fusion Energy Targets
Nov. 2002

NIFS-764
NIFS Contributions to 19th IAEA Fusion Energy Conference (Lyon, France, 14-19 October 2002)
Nov. 2002

NIFS-765 S. Goto and S. Kida
Enhanced Stretching of Material Lines by Antiparallel Vortex Pairs in Turbulence
Dec. 2002

NIFS-766 M. Okamoto, A.A. Maluckov, S. Satake, N. Nakajima and H. Sugama
Transport and Radial Electric Field in Torus Plasmas
Dec. 2002

NIFS-767 R. Kanno, N. Nakajima, M. Okamoto and T. Hayashi
Computational Study of Three Dimensional MHD Equilibrium with m/n=1/1 Island
Dec. 2002

NIFS-768 M. Yagi, S.-I. Itoh, M. Kawasaki, K. Itoh and A. Fukuyama
Multiple-Scale Turbulence and Bifurcaion
Jan. 2003

NIFS-769 S.-I. Itoh, K. Itoh and S. Toda
Statistical Theory of L-H Transition and its Implication to Threshold Database
Jan. 2003

NIFS-770 K. Itoh
Summary: Theory of Magnetic Confinement
Jan. 2003

NIFS-771 S.-I. Itoh, K. Itoh and S. Toda
Statistical Theory of L-H Transition in Tokamaks
Jan. 2003

NIFS-772 M. Stepic, L. Hadzievski and M.M. Skoric
Modulation Instability in Two-dimensional Nonlinear Schrodinger Lattice Models with Dispersion and Long-range Interactions
Jan. 2003

NIFS-773 M.Yu. Isaev, K.Y. Watanabe, M. Yokoyama and K. Yamazaki
The Effect of Hexapole and Vertical Fields on α-particle Confinement in Heliotron Configurations
Mar. 2003

NIFS-774 K. Itoh, S.-I. Itoh, F. Spineanu, M.O. Vlad and M. Kawasaki
On Transition in Plasma Turbulence with Multiple Scale Lengths
May 2003

NIFS-775 M. Vlad, F. Spineanu, K. Itoh, S.-I. Itoh
Intermittent and Global Transitions in Plasma Turbulence
July 2003

NIFS-776 Y. Kondoh, M. Kondo, K. Shimoda, T. Takahashi and K. Osuga
Innovative Direct Energy Conversion Systems from Fusion Output Thermal Power to the Electrical One with the Use of Electronic Adiabatic Processes of Electron Fluid in Solid Conductors.
July 2003